Res. (S) **1980**, 36–37; d) K. J. McCullogh, A. R. Morgan, D. C. Nonhebel, P. L. Pauson, *J. Chem. Res. (M)* **1980**, 651–676.
[27] F. L. Schadt, P. von R. Schleyer, T. W. Bentley, *Tetrahedron Lett.* **1974**, 2335–2338.
[28] L. Eberson, M. P. Hartshorn, J. J. McCullough, O. Persson, F. Radner, *Acta Chem. Scand.* **1998**, *52*, 1024–1028.
[29] L. Eberson, M. P. Hartshorn, O. Persson, F. Radner, *Chem. Commun.* **1996**, 2105–2112.
[30] P. Deslongchamps, *Stereoelectronic Effects in Organic Chemistry*, Pergamon, Oxford, **1986**, pp. 72–84.

Ligand Rotation Distinguishes First- and Second-Generation Ruthenium Metathesis Catalysts**

Christian Adlhart and Peter Chen*

We report herein a combined quantum mechanical/molecular mechanics (QM/MM) study of the olefin-metathesis reaction catalyzed by ruthenium carbene complexes. The discovery and progressive improvement of Ru-based metathesis catalysts[1] makes an understanding of the mechanistic basis for the high activity and broad substrate tolerance of considerable theoretical as well as practical interest. The discovery of the "first-generation" metathesis catalysts $[(Cy_3P)_2(Cl)_2Ru{=}CHPh]$ (**1**, Cy = cyclohexyl) by Grubbs and co-workers,[2] of which **1** is representative, and the subsequent discovery of the "second-generation" catalysts **2** by the groups of Grubbs,[3] Nolan,[4] and Herrmann,[5] in which an *N*-heterocyclic carbene (NHC) ligand replaces one phosphane group in the first-generation systems, has spurred the synthesis of even more varied structural variants as well as extensive mechanistic work. Recently, Grubbs and co-workers presented an extensive in situ kinetic study[6] in which it was concluded that the origin of the greatly increased activity in the second-generation catalysts derived from a more favorable branching ratio for the partitioning of the active carbene complex, ($[(L)(Cl)_2Ru{=}CHR]$, L = Cy_3P or NHC), between entry into the catalytic cycle and rebinding of a phosphane. We have reported gas-phase mechanistic studies[7,8] with substituent and isotope effects aimed at identifying the rate-determining step as well as the role of preequilibria in determining catalyst activity.

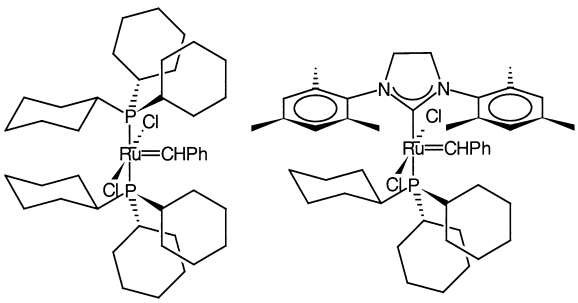

1 **2**

This growing body of experimental work on metathesis catalysts makes a computational study timely, particularly given the recent successes of mixed quantum-mechanical/classical methods (QM/MM) that allow a reasonable treatment of large organometallic complexes with explicit inclusion of the full ligand set[9] with conformational flexibility. Our calculations show that the first-generation catalysts **1** have a high barrier in the middle of the reaction coordinate imposed by the necessity of rotation of the threefold symmetric phosphane ligand; a comparable barrier is absent in second-generation catalysts **2** because of the twofold symmetry of the NHC ligand. Depending on whether the metathesis reaction is exothermic, thermoneutral, or endothermic, the rate-determining step should therefore change.

Calculations were carried out on the metathesis reaction of both **1** and **2** using the IMOMM approach[10] implemented in the ADF2000.02 (ADF = Amsterdam Density Functional) package[11] on Quant-X Alpha (Compaq Unix Tru64 Unix 5.3) and AMD Athlon (Red Hat Linux 7.1) machines. The QM model was the $[(Me_3P)_2(Cl)_2Ru{=}CHPh]$ unit with hydrogen atoms as dummies for the carbon atoms of the actual complexes. The α values[12] were obtained by full DFT calculations on the QM model units and the full complexes. A triple-ζ basis set was used on ruthenium;[13] a polarized double-ζ basis set was used for all other elements. The $1s^2 2s^2 2p^6 3s^2 3p^6 3d^{10}$ electrons of the ruthenium atoms, the $1s^2 2s^2 2p^6$ electrons of the chlorine and phosphorus atoms, and the $1s^2$ electrons of the carbon atoms were treated within a frozen-core approximation. A set of auxiliary s, p, d, f, and g STO functions (STO = Slater orbital) centered on all nuclei was used to fit the molecular density and present Coulomb and exchange potentials accurately in each SCF cycle (SCF = self-consistent field).[13] The local density approximation by Vosko, Wilk, and Nusair,[14] and generalized gradient approximation were used with the BP86 functional.[15] Scalar relativistic corrections were added to the total energy.[16] Because all systems investigated showed a large HOMO–LUMO gap, a spin-restricted formalism could be employed throughout. For the MM part of the calculation, a modified sybyl/tripos 5.2 force field[17] was implemented.[18] In the course of comparing QM/MM to full DFT energies, we noticed that there was a systematic error that could be traced back to a double counting of MM interactions. Therefore the MM contribution to the hybrid DFT/MM energy has been removed, as most of this interaction is already taken into account by the imposed strain of the MM system on the DFT system. Validation against full DFT energies at full DFT-optimized structures show that the QM/MM energies simulate full DFT values to within 3–4 kcal mol^{-1} in the worst case; the agreement is often much better. The conformational space,

[*] Prof. Dr. P. Chen, C. Adlhart
Laboratorium für Organische Chemie, ETH Hönggerberg
8093 Zürich (Switzerland)
Fax: (+41) 1-632-1280
E-mail: chen@org.chem.ethz.ch

[**] We acknowledge helpful discussions with Professor U. Röthlisberger and Dr. A. Magistrato in implementing QM/MM calculations in our group. This project was supported by the Swiss National Science Foundation and the Research Commission of the ETH Zürich.

Supporting information for this article is available on the WWW under http://www.angewandte.org or from the author.

  0044-8249/02/4123-4484 $ 20.00+.50/0

especially with regard to the cyclohexyl rings, was systematically searched. When X-ray structures were available, the optimized QM/MM structures were found to be in excellent agreement.[19]

Transition states were approached by a linear transit from the reactant to the product and from the product to the reactant by calculation of a series of structures constrained to a particular value of the geometric parameter corresponding to the reaction coordinate (the C–C distances in the metallacyclobutane or the Cl-Ru-P-C torsional angle for PCy_3 rotation) with unconstrained optimization of all other geometric parameters. As a further check for each transition state, the geometries were then relaxed in both forward and reverse directions to confirm that they converge to the reactants and products (or intermediates in the case of PCy_3 rotation, which shows several transition states).[20] With full DFT validation at the important critical points, the potential surfaces for the metathesis reactions with **1** and **2** were explored widely with QM/MM. In contrast to previous studies,[8,21] the steric effects of the very large ligands (Tolman cone angles[22] for PCy_3, PMe3, and PH_3 are 170°, 118° and 87°, respectively) can be explicitly treated; these steric effects are, in fact, critical to the conclusion of this study (see below).

The results for the degenerate metathesis of styrene with **1** are shown in Figure 1. Alternative reaction pathways involving *cis* dichloro complexes, as well as an associative ligand exchange of an olefin for phosphane were calculated and found to be less favorable.[20] Similar surfaces for the metathesis of simple olefins with **2**, and the metathesis of ethyl vinyl ether with **1** and **2**, were also calculated.[20] Grubbs and co-workers reported enthalpies of activation for phosphane exchange of 23.6 ± 0.5 kcal mol (with **1**) and 27 ± 2 kcal mol^{-1} (with **2**).[6] These values agree gratifyingly well with the calculated full DFT values of 20.8 and 28.0 kcal mol^{-1}, as well as with the QM/MM results. The reaction coordinate in Figure 1 is representative of a thermoneutral metathesis reaction with a first-generation catalyst. Rotation of the tricyclohexylphosphane in any of the structures is primarily hindered by the unfavorable steric interaction with the large chlorine atoms. The barrier of rotation for PH_3 was calculated to be only 0.16 kcal mol^{-1}, illustrating the very large difference between PH_3 and PCy_3 (6.0 kcal mol^{-1}). In other studies, rotation barriers between 7 and 18 kcal mol^{-1} were found for bulky phosphanes.[23] The potential surface for the metathesis of ethyl vinyl ether, calculated to be exothermic by 9.45 kcal mol^{-1}, is very similar to that in Figure 1 for structures **I**–**IV**′. The exothermicity appears only upon cleavage of the metallacyclobutane, meaning that transition states from **IV** to **VI** or from **IV**′ to **III**′, are the first structures to be substantially lowered in energy—all subsequent structures are also lowered.

For second-generation catalysts **2**, the potential surface is much simpler; a cursory examination of the structure analogous to **IV** shows that no rotation is needed because the NHC ligand has only twofold symmetry, as opposed to the threefold symmetry of the phosphane ligand in **1**. As mentioned above, the calculated barrier for phosphane dissociation from **2** agrees well with the experimental value. The structures **II**–**IV** (analogous to **2**) for the metathesis of ethylene have calculated energies (full DFT) of 28.0, 14.6, and 12.9 kcal mol^{-1}, respectively; the rest of the surface would be the mirror image of **IV**–**I** in the case of a thermoneutral metathesis reaction.

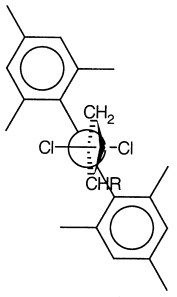

analogue of **IV**

Our calculations, which establish the gross topology of the potential surfaces, should substantially facilitate the interpretation of experimental mechanistic studies. Given that the QM/MM method reproduces QM energies to within 3–4 kcal mol^{-1}, and given the (previously unknown) accuracy of even a full DFT calculation, good agreement with experimental data is found,[8] if one presumes that the transition state for **IV**→**VI** lies, in reality, slightly higher in energy that that for **IV**→**IV**′; the two transition states differ by less than 1 kcal mol^{-1} in the QM/MM calculation. For near-thermoneutral metathesis reactions with first-generation catalysts, the rate-determining step would then be ligand rotation at the metallacyclobutane structure. For strongly exothermic metathesis reactions, for example, vinyl ethers, lowering of the energy of the transition state for **IV**→**VI**, but not that for **IV**→**IV**′, by strain release would allow rotation to occur at a later stage.

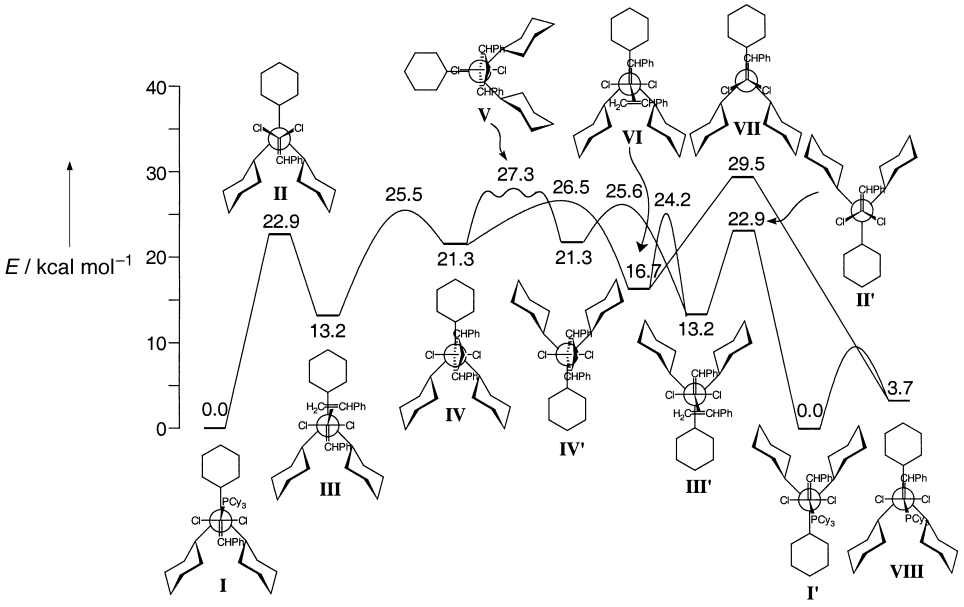

Figure 1. Reaction coordinate for the degenerate metathesis of styrene with **1** as catalyst; the values are QM/MM energies in kcal mol^{-1}. Free ligands needed for mass balance are not shown but were included in the calculation. Complex **1** is depicted in a Newman-like projection viewed along the P–Ru bond to emphasize conformational differences.

  0044-8249/02/4123-4485 $ 20.00+.50/0

Metallacyclobutane formation becomes rate-limiting in the exothermic case.

Nevertheless, the transition state for **III**→**IV** remains higher than that for phosphane dissociation in the first-generation catalysts. In metathesis reactions with second-generation, a higher barrier is found for phosphane dissociation, whereas the barrier for metallacyclobutane formation is comparable to that in the first-generation systems. Phosphane dissociation is always rate-limiting for second-generation catalysts. These conclusions are completely consistent with the experimental findings of Grubbs and co-workers in the metathesis of ethyl vinyl ether,[6] although the nature of the barriers after phosphane dissociation was not identified in that work. Moreover, the gas-phase results from our group[8] are also consistent with the calculated surfaces. In that work, we interpreted substituent and isotope effects as indicating that the metallacyclobutane structure must be the rate-determining transition state. A more appropriate formulation would be to say that the rate-determining transition state in first-generation catalysts has a metallacyclobutane structure, which is not exactly the same statement, but is now fully supported by experiment and theory.

It is clear that electronic effects[6,21] have a significant effect on the precise height of the barrier for phosphane dissociation. The major topological differences between the potential surfaces for first- and second-generation metathesis catalysts can be traced to the different symmetries of the phosphane and the NHC ligands. We propose that high barriers on the potential surface after the phosphane dissociation can be eliminated by choosing ligands with twofold as opposed to threefold symmetry. A concrete test of the proposal will be provided by a next-generation ruthenium metathesis catalyst in which the tricyclohexylphosphane ligands in **1** are replaced by 2,5-diarylphosphabenzene ligands similar to those prepared by Breit et al.[24] for rhodium hydroformylation catalysts. The complex combines the advantages of the first- and second-generation catalysts: the complex should show both a reduced barrier for dissociation of the remaining phosphane *and* a favorable partitioning of the olefin π-complex towards the product. The synthesis and characterization of the new catalyst is underway.

Received: May 16, 2002 [Z19321]

[1] K. J. Ivin, J. C. Mol, *Olefin Metathesis and Metathesis Polymerization*, Academic Press, San Diego, **1997**; T. M. Trnka, R. H. Grubbs, *Acc. Chem. Res.* **2001**, *34*, 18; A. Fürstner, *Angew. Chem.* **2000**, *112*, 3140; *Angew. Chem. Int. Ed.* **2000**, *39*, 3012; R. H. Grubbs, S. Chang, *Tetrahedron* **1998**, *54*, 4413.

[2] S. T. Nguyen, L. K. Johnson, R. H. Grubbs, J. W. Ziller, *J. Am. Chem. Soc.* **1992**, *114*, 3974.

[3] J. P. Morgan, R. H. Grubbs, *Org. Lett.* **2000**, *2*, 3153; M. Scholl, S. Ding, C. W. Lee, R. H. Grubbs, *Org. Lett.* **1999**, *1*, 953; M. Scholl, T. M. Trnka, J. P. Morgan, R. H. Grubbs, *Tetrahedron Lett.* **1999**, *40*, 2247.

[4] J. Huang, E. D. Stevens, S. P. Nolan, J. L. Peterson, *J. Am. Chem. Soc.* **1999**, *121*, 2674.

[5] T. Weskamp, F. J. Kohl, W. Hieringer, D. Gleich, W. A. Herrmann, *Angew. Chem.* **1999**, *111*, 2573; *Angew. Chem. Int. Ed.* **1999**, *38*, 2416.

[6] M. S. Sanford, M. Ulman, R. H. Grubbs, *J. Am. Chem. Soc.* **2001**, *123*, 749; M. S. Sanford, J. A. Love, R. H. Grubbs, *J. Am. Chem. Soc.* **2001**, *123*, 6543.

[7] C. Adlhart, M. A. O. Volland, P. Hofmann, P. Chen, *Helv. Chim. Acta* **2000**, *83*, 3306; C. Adlhart, P. Chen, *Helv. Chim. Acta* **2000**, *83*, 2192; C. Hinderling, C. Adlhart, P. Chen, *Angew. Chem.* **1998**, *110*, 2831; *Angew. Chem. Int. Ed.* **1998**, *37*, 2685.

[8] C. Adlhart, C. Hinderling, H. Baumann, P. Chen, *J. Am. Chem. Soc.* **2000**, *122*, 8204.

[9] J. Vasquez, B. Goldfuss, G. Helmchen, *J. Organomet. Chem.* **2002**, *641*, 67; L. Cavallo, M. Sola, *J. Am. Chem. Soc.* **2001**, *123*, 12294; M. A. Esteruelas, A. Lledos, M. Martin, F. Maseras, R. Oses, N. Ruiz, J. Tomas, *Organometallics* **2001**, *20*, 5297; S. A. Decker, T. R. Cundari, *J. Organomet. Chem.* **2001**, *635*, 132; J. J. Carbo, F. Maseras, C. Bo, P. W. N. M. van Leeuwen, *J. Am. Chem. Soc.* **2001**, *123*, 7630; A. Macchioni, C. Zuccaccia, E. Clot, K. Gruet, R. H. Crabtree, *Organometallics* **2001**, *20*, 2367; S. Feldgus, C. R. Landis, *Organometallics* **2001**, *20*, 2374; E. Jacobsen, L. Cavallo, *Chem. Eur. J.* **2001**, *7*, 800; P. Longo, F. Grisi, G. Guerra, L. Cavallo, *Macromolecules* **2000**, *33*, 4647; T. K. Woo, G. Pioda, U. Röthlisberger, A. Togni, *Organometallics* **2000**, *19*, 2144; B. Goldfuss, M. Steigelmann, F. Rominger, *Eur. J. Org. Chem.* **2000**, 1785; T. K. Woo, P. E. Blochl, T. Ziegler, *J. Phys. Chem. A* **2000**, *104*, 121; B. Goldfuss, M. Steigelmann, S. I. Khan, K. N. Houk, *J. Org. Chem.* **2000**, *65*, 77; D. Gleich, W. A. Herrmann, *Organometallics* **1999**, *18*, 4354; G. Ujaque, F. Maseras, A. Lledos, *J. Am. Chem. Soc.* **1999**, *121*, 1317; A. C. Cooper, E. Clot, J. C. Huffman, W. E. Streib, F. Maseras, O. Eisenstein, K. G. Caulton, *J. Am. Chem. Soc.* **1999**, *121*, 97; L. Cavallo, T. K. Woo, T. Ziegler, *Can. J. Chem.* **1998**, *76*, 1457; D. Gleich, R. Schmid, W. A. Herrmann, *Organometallics* **1998**, *17*, 4828; J. Jaffart, R. Mathieu, M. Etienne, J. E. McGrady, O. Eisenstein, F. Maseras, *Chem. Commun.* **1998**, 2011; L. Q. Deng, T. Ziegler, T. K. Woo, P. Margl, L. Y. Fan, *Organometallics* **1998**, *17*, 3240; L. Q. Deng, T. K. Woo, L. Cavallo, P. M. Margl, T. Ziegler, *J. Am. Chem. Soc.* **1997**, *119*, 6177.

[10] F. Maseras, K. Morokuma, *J. Comput. Chem.* **1995**, *16*, 1170.

[11] G. T. Velde, F. M. Bickelhaupt, E. J. Baerends, C. F. Guerra, S. J. A. van Gisbergen, J. G. Snijders, T. Ziegler, *J. Comput. Chem.* **2001**, *22*, 931.

[12] For each covalent bond that crosses the QM/MM boundary, there is one atom that lies on the MM side of the partition and one atom that lies on the QM side. For each of these link bonds, a dummy hydrogen atom is used to cap the electronic system. The link bond is constrained to lie along the dummy bond vector such that the ratio, $\alpha = |R_{\mathrm{link}}|/|R_{\mathrm{dummy}}|$ (R = bond length) is constant. The ratio α used in the calculations was determined by comparing the bond lengths in the full QM calculation of **1** with the equivalent bond lengths of the dummy bonds in the model and then taken as the average. We find $\alpha = 1.3971 \pm 0.0013$.

[13] J. G. Snijders, E. J. Baerends, P. Vernoijs, *At. Data Nucl. Data Tables* **1981**, *26*, 483; P. Vernoijs, J. G. Snijders, E. J. Baerends, *Slater Type Basis Functions for the Whole Periodic System*, Department of Theoretical Chemistry, Free University of Amsterdam, **1981**; J. Krijn, E. J. Baerends, *Fit Functions in the HFS Method*, Department of Theoretical Chemistry, Free University of Amsterdam, **1984**.

[14] S. Vosko, M. Wilk, M. Nusair, *Can. J. Phys.* **1980**, *58*, 1200.

[15] A. D. Becke, *Phys. Rev. A* **1988**, *38*, 3098; J. P. Perdew, *Phys. Rev. B* **1986**, *33*, 8822.

[16] J. G. Snijders, E. J. Baerends, *Mol. Phys.* **1979**, *36*, 1789; J. G. Snijders, E. J. Baerends, P. Ros, *Mol. Phys.* **1978**, *38*, 1909.

[17] M. Clark, R. Cramer III, N. van Opdenbosch, *J. Comp. Chem.* **1989**, *10*, 982.

[18] Modifications for Ru: $E_{\mathrm{bond}} = 0.5\,K(r-r_0)^2$; $K = 600$; r(Ru-P3) = 2.436; r(Ru-Cl) = 2.400; (Ru-C2) = 1.839; $E_{\mathrm{bend}} = 0.5\,K(\theta-\theta_0)^2$; $K = 200$; θ(Ru-P3-C3) = 119.2; θ(Cl-Ru-P3) = 87.2; θ(C2-Ru-Cl) = 88.7; θ(C2-Ru-P3) = 101.1; θ(Cl-Ru-Cl) = 167.6; $E_{\mathrm{torsion}} = 0.5\,K(1 + \mathrm{per}\cos(\mathrm{per}\,\phi))$; for C2-Ru-P3-C3, Cl-Ru-P3-C3, and P3-Ru-P3-C3, $K = 0.2740$ and per = 3.0; van der Waals parameters for Ru: $E_{\mathrm{min}} = 0.56$; $r_{\mathrm{min}} = 2.963$; $\alpha = 12.0$.

[19] Root-mean-square deviation of bond distances [Å], bond angles [deg], and torsional angles [deg]: crystal QM/MM: 0.028 ± 0.0032, 1.2 ± 0.32, 4.2 ± 2.0; crystal, DFT: 0.017 ± 0.0042, 0.8 ± 0.22, 1.6 ± 0.53; QM/MM, DFT: 0.016 ± 0.0027, 0.8 ± 0.25, 3.9 ± 1.75. Reference for crystal of $[(Cy_3P)_2(Cl)Ru{=}CH(p\text{-}C_6H_4Cl)]$: P. Schwab, M. B. France, J. W. Ziller, R. H. Grubbs, *Angew. Chem.* **1995**, *107*, 2179; *Angew. Chem. Int. Ed. Engl.* **1995**, *34*, 2039.

  0044-8249/02/4123-4486 $ 20.00+.50/0

[20] A full account of the calculations with structures and energies for all of the examined cases, that is, the search of conformational space, is in preparation. Cartesian coordinates and energies for validation for all structures reported herein are given in the Supporting Information.
[21] O. M. Aagaard, R. J. Meier, F. Buda, *J. Am. Chem. Soc.* **1998**, *120*, 7174; R. J. Meier, O. M. Aagaard, F. Buda, *J. Mol. Catal. A* **2000**, *160*, 189; S. F. Vyboishchikov, M. Bühl, W. Thiel, *Chem. Eur. J.* **2002**, *8*, 3962..
[22] C. A. Tolman, *Chem. Rev.* **1977**, *77*, 313.
[23] J. W. Faller, B. V. Johnson, *J. Organomet. Chem.* **1975**, *96*, 99; W. D. Jones, F. J. Feher, *Inorg. Chem.* **1984**, *23*, 2376; J. Polowin, M. C. Baird, *J. Organomet. Chem.* **1994**, *478*, 45; F. P. Fanizzi, M. Lanfranchi, G. Natile, A. Tiripicchio, *Inorg. Chem.* **1994**, *33*, 3331; J. Albert, R. Bosque, J. M. Cadena, S. Delgado, J. Granell, *J. Organomet. Chem.* **2001**, *634*, 83.
[24] B. Breit, R. Winde, T. Mackewitz, R. Paciello, K. Harms, *Chem. Eur. J.* **2001**, *7*, 3106; B. Breit, *J. Mol. Catal. A* **1999**, *143*, 143; B. Breit, R. Winde, K. Harms, *J. Chem. Soc. Perkin Trans. 1* **1997**, 2681.

Solvothermal Synthesis, Crystal Structure, Thermal Stability, and Mössbauer Spectroscopic Investigation of the Mixed-Valent Thioantimonate(III,V) $[Ni(dien)_2]_2Sb_4S_9$**

Ralph Stähler, Bernd-Dieter Mosel, Hellmut Eckert, and Wolfgang Bensch*

During the last decade it was impressively demonstrated by several groups that the solvothermal technique is not only a promising route for the preparation of new and exciting open framework oxidic compounds but also for the syntheses of fascinating thio- and selenometalates.[1–7] Since the pioneering work of Schäfer and co-workers,[8] about 50 new thioantimonates have been prepared and characterized. In most compounds antimony occurs as Sb^{III} and, because of the variable coordination behavior caused by the stereochemically active lone pair),[9] the dimensionalities of the anionic Sb_xS_y frameworks range over 1D chains, 2D layers, and 3D interconnection of the SbS_x primary building units. Thioantimonates(v) always contain tetrahedral $[Sb^VS_4]^{3-}$ ions that are not further interconnected or condensed. To date the coexistence of Sb^{III} and Sb^V within a polymeric thioantimonate anion was never observed.

Normally solvothermal syntheses are performed using organic molecules as structure-directors. Recently, we demonstrated that transition-metal complexes can also be used as "template" molecules[11–13,15–18]. During our systematic experiments with the in situ formed $[Ni(dien)_2]^{2+}$ ion (dien = diethylenetriamine) as the structure-directing molecule, we synthesized and fully characterized the first mixed-valent thioantimonate anion $^1_\infty[Sb_4S_9]^{4-}$ which contains Sb^{III} and Sb^V. The title compound was obtained under solvothermal conditions as yellow polyhedra that are stable to air, in water, and in acetone. The results of a large number of syntheses performed at different temperatures and for different reaction times suggest that the $[Ni(dien)_2]_2Sb_4S_9$ is formed at higher temperatures and in short reaction times. The compound crystallizes in the monoclinic space group $P2_1/c$.[10]

The $^1_\infty[Sb_4S_9]^{4-}$ ion is composed of three $Sb^{III}S_3$ pyramids (Sb2, Sb3, and Sb4), which share common corners leading to the formation of an Sb_3S_7 moiety (Figure 1). The Sb1 atom is in a tetrahedral coordination environment of four S atoms to form a Sb^VS_4 tetrahedron. The interconnection of the Sb_3S_7 unit and the Sb^VS_4 tetrahedron through the S4 atom yields the $[Sb_4S_9]^{4-}$ ionic chain. The bond lengths in the $Sb^{III}S_3$ units are between 2.331(1) and 2.637(1) Å, with S-Sb^{III}-S angles ranging from 88.33(3) to 102.21(4)°. The longest Sb–S bond is between Sb2 and S4 joining the Sb_3S_7 and SbS_4 units.

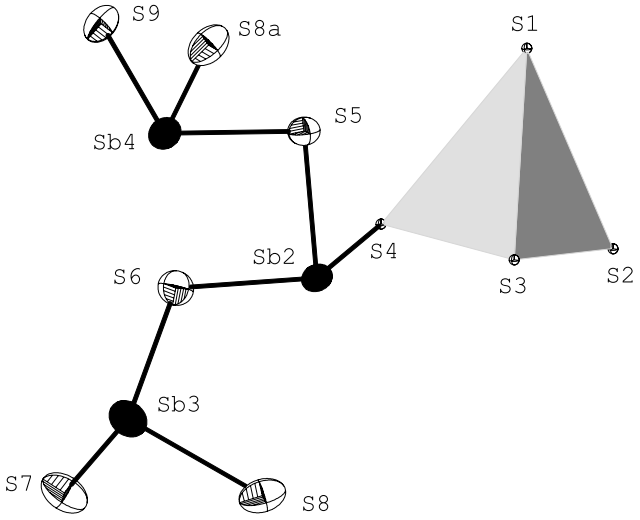

Figure 1. The $^1_\infty[Sb_4S_9]^{2-}$ ion with labelling. The Sb^VS_4 unit is shown as a tetrahedron. The displacement ellipsoids are drawn at the 50 % probability level. Selected bonds angles [°]: S1-Sb1-S2 113.64(4), S1-Sb1-S3 110.33(4), S1-Sb1-S4 110.36(4), S2-Sb1-S3 109.86(4), S2-Sb1-S4 106.02(4), S3-Sb1-S4 106.30(4). Symmetry code for S8a: $-x$, $-0.5+y$, $0.5-z$.

The Sb^{III}–S interatomic distances, as well as the angles, are in the range reported in the literature.[2,5,7,11–15] The Sb^V1–S interatomic distances are significantly shorter than Sb^{III}–S bonds and vary between 2.294(1) and 2.390(1) Å, with S-Sb1-S angles ranging from 106.02(4) to 113.64(4)°, which indicate only a slight deviation from the ideal tetrahedral geometry. Sb^V1–S interatomic distances and S-Sb^V-S angles are in the range found in the literature.[12,16,17] The anionic chains have a sinusoidal shape and run along [010] (Figure 2). The Sb^VS_4 tetrahedra are located at the exterior of the central Sb_3S_7 backbone of the anion. The compound decomposes in two steps starting at about $T_{onset} = 257$ °C, as evidenced by differential thermal analysis–thermogravimetric analysis–

[*] Prof. Dr. W. Bensch, Dipl.-Chem. R. Stähler
Institut für Anorganische Chemie
Universität Kiel
Olshausenstrasse 40, 24098 Kiel (Germany)
Fax: (+49) 431–880–1520
E-mail: wbensch@ac.uni-kiel.de
Dr. B.-D. Mosel, Prof. Dr. H. Eckert
Institut für Physikalische Chemie
Westfälische Wilhelms-Universität Münster
Schlossplatz 7, 48149 Münster (Germany)

[**] This work was supported by the States of Schleswig-Holstein and Nordrhein-Westfalen, and the Fonds der Chemischen Industrie. dien = diethylenetriamine.

  0044-8249/02/4123-4487 $ 20.00+.50/0